

SARS-CoV-2 infection in the central nervous system of a 1-year-old infant submitted to complete autopsy

Ismael Gomes^{1,3*}, Karina Karmirian^{2,3*}, Júlia Oliveira^{2*}, Carolina Pedrosa^{2*}, Fernando Colonna Rosman^{1,5}, Leila Chimelli⁴, Stevens Rehen^{2,3}

*These authors contributed equally to this work

Corresponding authors:

Stevens Rehen (srehen@lance-ufrj.org)

Leila Chimelli (lcneuropatologia@gmail.com)

Affiliation details:

1 - Anatomic Pathology Service, Jesus Municipal Hospital, Rio de Janeiro, RJ, Brazil.

2 – D’Or Institute for Research and Education (IDOR), Rio de Janeiro, Brazil.

3 – Institute of Biomedical Sciences, Federal University of Rio de Janeiro (UFRJ), Rio de Janeiro, Brazil.

4 - Laboratory of Neuropathology, State Institute of Brain Paulo Niemeyer, Rio de Janeiro, RJ, Brazil.

5 - Department of Pathology, Faculty of Medicine, Federal University of Rio de Janeiro (UFRJ), Rio de Janeiro, Brazil.

Summary

Coronavirus disease 2019 (COVID-19) was initially characterized as a respiratory illness. Neurological manifestations were reported mostly in severely affected patients. Routes for brain infection and the presence of virus particles in situ have not been well described, raising controversy about how the virus causes neurological symptoms. Here, we report the autopsy findings of a 1-year old infant with COVID-19. In addition to pneumonitis, meningitis and multiple organ damage related to thrombosis, a previous encephalopathy may have contributed to additional cerebral damage. SARS-CoV-2 infected the choroid plexus, ventricles, and cerebral cortex. This is the first evidence of SARS-CoV-2 detection in an infant post-mortem brain.

Introduction

COVID-19 is caused by a Severe Acute Respiratory Syndrome Coronavirus 2 (SARS-CoV-2). Emerged in Wuhan, China, in December 2019, the virus speedily spread globally and has infected more than 23 million people, causing 817,000 deaths until late August 2020 (1). With about 35,000 new cases per day worldwide (1), SARS-CoV-2 poses a threat to health systems, especially in countries where the spread of virus was still not mitigated.

COVID-19 is mainly characterized by respiratory signs and symptoms, however, affected patients can develop acute and chronic neurological symptoms, like headache, dizziness, hypogeusia and hyposmia (2), and clinical impairments, such as persistent fatigue (3) and meningitis/encephalitis (4).

Neurotropism seems to be one of the characteristics of the coronavirus family. Brain samples of a patient that developed SARS presented particles of SARS-CoV, besides an extensive neuronal necrosis and broad glial hyperplasia (5). However, the presence of the SARS-CoV-2 in the nervous system has not yet been described. The SARS-CoV-2 RNA had already been reported in cerebrospinal fluid of one patient with viral encephalitis (4). Brain sections of 18 patients were evaluated by quantitative RT-PCR for SARS-CoV-2 and presented low levels of RNA only in 3 sections from the medulla and 3 from the frontal lobe/olfactory nerves (6) of 5 patients. A microscopic examination of these samples revealed loss of neurons in the cerebral cortex, hippocampus, and cerebellum (6).

Here, we describe the pathological alterations associated with the presence of SARS-CoV-2 in post-mortem tissues of a 1-year and 2-months-old infant, who died from respiratory failure caused by COVID-19.

Case Report

A female infant born in February 2019, at term, healthy, and with normal neurological development, was admitted to an emergency hospital in December 2019 presenting vomits, hypotonia, and seizures. The clinical hypothesis was viral meningitis, although a cerebrospinal fluid (CSF) cytology examination has not been performed. After 16 days, she was discharged without sequelae except for sporadic episodes of convulsive seizures. Since February 2020, she was hospitalized three times. In early April she was readmitted to the hospital presenting vomits and repetitive movements in the left upper and lower limbs, hypotonia, postural instability, and inability to support her head, to seat, to walk, and the auscultation of the respiratory system revealing universally audible vesicular murmur, wheezing, rhonchi, and rales. She evolved with intermittent periods of dyspnea, tachypnea, and use of accessory muscles to breathe, along with tachycardia and fever, anemia, leukocytosis, and relative lymphopenia and neutrophilia. She also presented elevated alanine aminotransferase, aspartate aminotransferase and C-reactive protein, normal bilirubin, and metabolic acidosis and respiratory alkalosis, requiring oxygen therapy and assisted ventilation. The tracheal secretion tested positive for SARS-CoV-2 by RT-PCR, and the cranial computed tomography showed brain atrophy with compensatory hydrocephalus. She evolved to impaired consciousness (Glasgow scale 3), hemodynamic instability, and died twenty-five days after admission, due to respiratory failure caused by bilateral coronavirus pneumonitis.

Materials and Methods

Autopsy procedures and tissue processing

Full autopsy was performed with a post-mortem interval of 48 hours and following best practices autopsy guidelines, according to biosafety practices in Anatomical Pathology Laboratories. All tissues were fixed at 10% buffered formalin (pH 7.4) for at least 48 hours.

Tissue samples were processed using a standard protocol for paraffin embedding and 4- μ m sections were stained with Hematoxylin and Eosin (H&E). Immunohistochemistry was performed in selected areas of the nervous tissue which presented histological lesions using anti-glial fibrillary acidic protein (GFAP), anti-NeuN, CD3, and CD68 antibodies, according to routine procedures with further detection by DAB-peroxidase system.

For immunofluorescence and confocal imaging, paraffin blocks from lungs and brain (choroid plexus [ChP], cerebral cortex, lateral ventricle, medulla oblongata, midbrain, pons and putamen) were

selected to produce a tissue microarray block, adapted from Pires et al. (7). Then, four μm sections were obtained and incubated with anti-SARS-CoV-2 spike protein monoclonal antibody (SP) overnight at 4°C , followed by Goat anti-Mouse Alexa Fluor 488 secondary antibody incubation. Nuclei were stained with $0.5 \mu\text{g/mL}$ 4'-6-diamino-2-phenylindole. The images were acquired with a confocal microscope Leica TCS SP8 using a 63x objective lens.

Further details of materials and methods are described in the Supplementary Material.

The research protocol was submitted for approval at the local Ethics Committee (Copa D'Or Hospital/Instituto D'Or de Pesquisa e Ensino, IDOR, CAAE number: 37211220.0.0000.5249), and was performed according to Declaration of Helsinki.

Results

Morphological findings

Macroscopic and histopathological examination revealed damages in multiple organs. As expected, coronavirus pneumonitis caused lung congestion and edema (**Figs 1 A1 and A2**); the interstitial inflammation delineated the pulmonary acini (**Fig 1 A2**). Histologically, it was characterized by some bronchial lymphoid aggregates, interstitial lymphocytic infiltrate, and diffuse damage of bronchioles, some of them covered with hyaline membranes, or containing eosinophilic plugs of plasma proteins and cellular debris, along with collapsed alveolar spaces (**Fig 1 A3**). In addition, there was congestion, edema, hemorrhagic foci, atelectasis, and recent microthrombi in some branches of pulmonary arteries in both lungs (**Supp Fig. 1A**).

A comprehensive analysis of the encephalic tissues was made. It showed severe cerebral atrophy and consequent large remaining space within the cranial cavity (**Fig 1 B1**). The brain weight (635 grams) was about 67% less than normal parameters (range weight: 940 to 1,010 grams). On sections, the cortical surfaces were thin, granulated and discolored (**Fig. 1 B2**). Histologically, pronounced damage was detected in many regions of the cerebral and cerebellar cortex, such as laminar cortical necrosis, spongiosis, microvascular proliferation and diffuse cerebral edema (**Figs 1 B3 and B4**). Severe cortical nerve cell loss was better detected with NeuN immunostaining (**Fig 2 A1 and A2**) with consequent severe reactive gliosis, also involving basal ganglia and the periventricular region (**Fig 2 B1-B5**) and microglial and macrophagic proliferation (**Fig 2 C1 and C2**). Lymphocytes were seen in the leptomeninges, particularly in the cerebellum (**Fig 1 B5**). They were fewer over the cerebral cortex and immunostained with CD3 (**Fig. 2 D**).

Other findings revealed venous and arterial microthrombosis in multiple organs, including small arteries in the lungs, kidneys and left ventricular myocardium (**Supp Figs 1A-C**). Venous thrombosis was pronounced in vascular structures related to thymus, esophagus, liver and thyroid (**Supp Figs 1D-G**). We also observed a focal pelvic thrombophlebitis (**Supp Fig 1H**) and a massive pancreatic ischemic necrosis secondary to venous or arterial thrombosis, along with extensive hemorrhage (**Supp Fig 1I**) without pancreatitis.

Other tissue injuries were observed, including esophagitis and tracheitis, with lymphocyte inflammatory infiltrate in the mucosa (**Supp Figs 2A-B**), laryngitis with necrosis and mucosal erosion, and hepatic steatosis (**Supp Figs 2C-D**). Morphological findings are summarized in **Supp Table 1**.

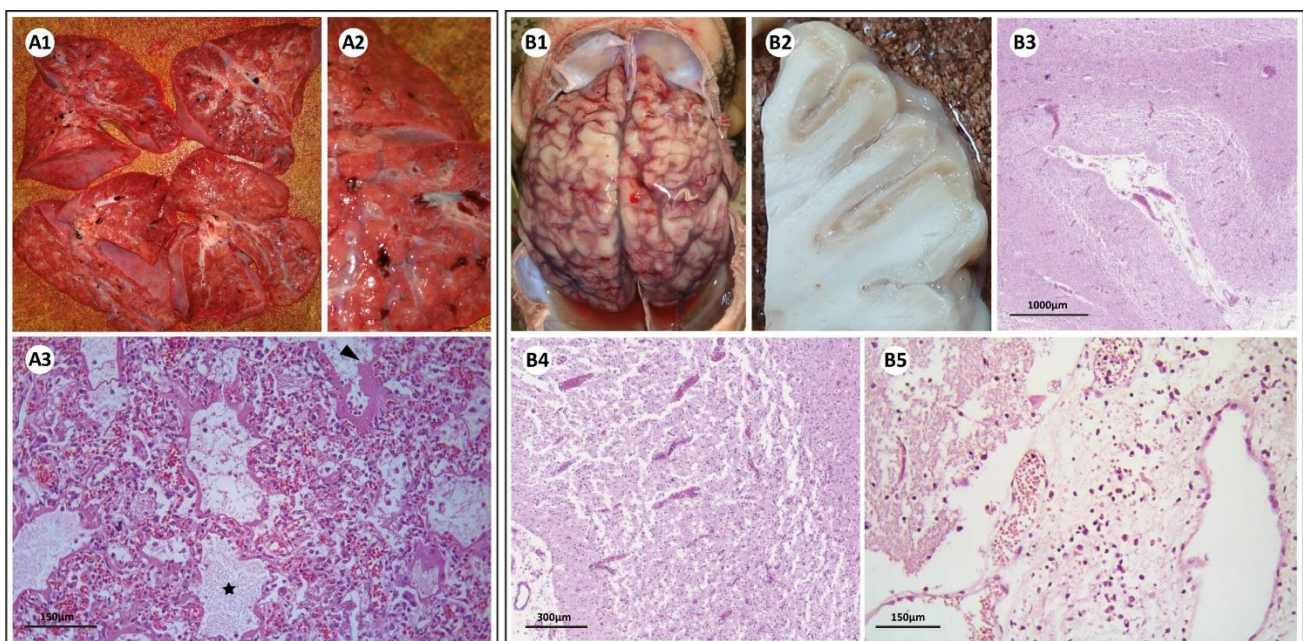


Figure 1: Macroscopic and microscopic appearances of brain and lungs. (A1) Cut surfaces of the left (above) and the right (below) congested and edematous lungs. In (A2) the pulmonary acini (lobules) are well delimited due to the pneumonitis. Post-mortem clots are seen in branches of pulmonary arteries. (A3) Diffuse damage of bronchioles (star), associated with eosinophilic hyaline membranes (arrowhead). Note the congestion of the alveolar capillaries, the collapsed alveolar spaces and the interstitial lymphocytic infiltrate. (B1) Unfixed brain in situ does not fill the base of the skull due to marked hypotrophy. (B2) Cut surface of fixed brain showing thin granular and discolored cortex. (B3) Histological section of cortex and white matter, showing cortical laminar necrosis. Detail in (B4). There is severe nerve cell loss and vascular proliferation, but the molecular layer (left) is relatively spared. (B5) Mild lymphocytic infiltration is seen in the cerebellar leptomeninges. (A3, B3, B4, B5 - H&E).

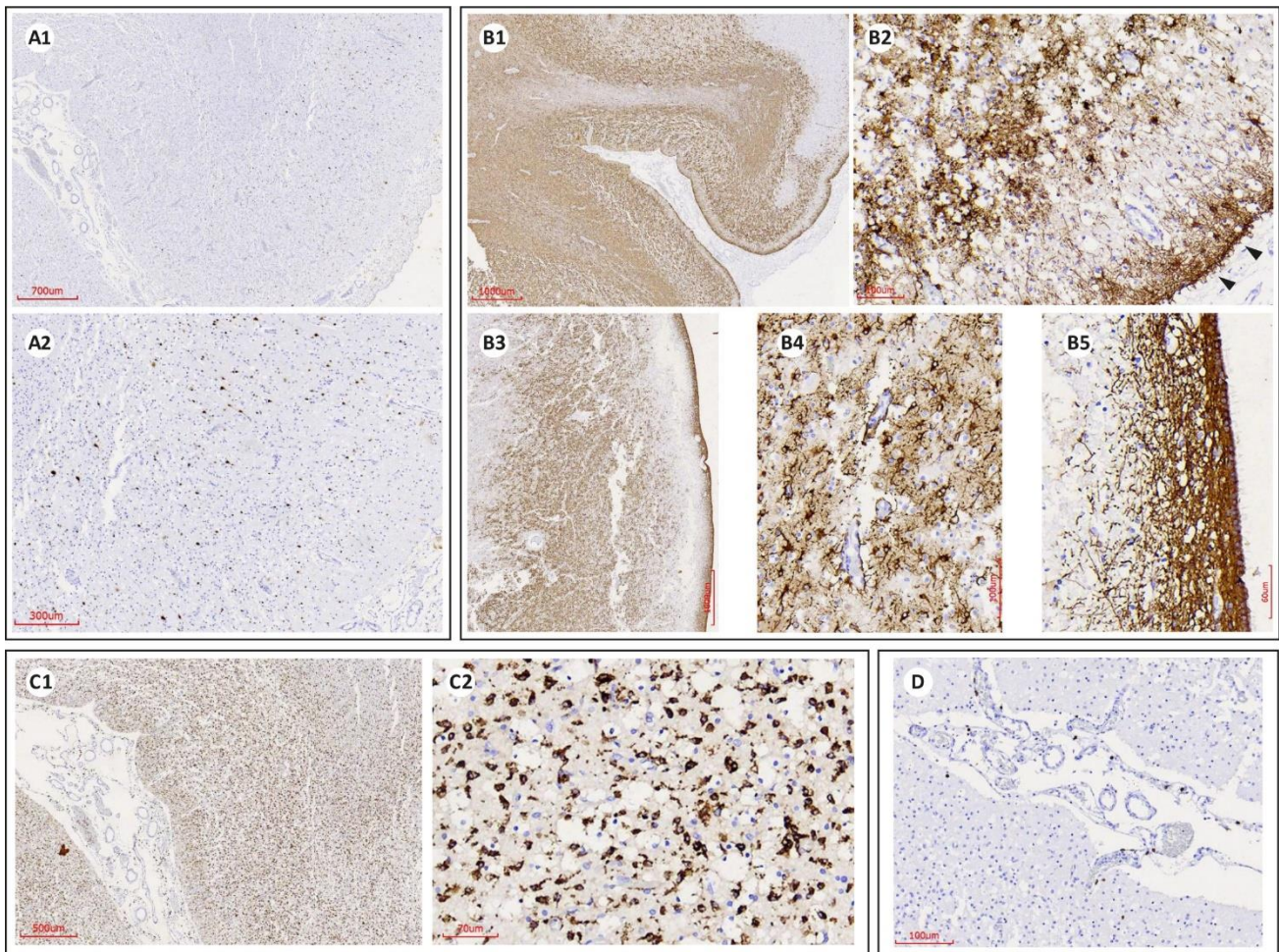


Figure 2: Immunostainings with NeuN (A), GFAP (B), CD68 (C), and CD3 (D). Severe cortical nerve cell loss (**A1**) compared with a transition with a better-preserved area (**A2**), where scattered pyramidal neurons are present. (**B1**) Severe reactive gliosis involving cortex and white matter except in an area where the cortical neurons (and axons in the corresponding white matter) have not been lost (upper right corner). A detail of the cortical gliosis is seen in (**B2**), including the subpial region (arrowheads), but sparing part of the molecular layer. (**B3**) Caudate nucleus and periventricular region including the ependymal surface with severe gliosis (details in **B4** and **B5**, respectively). (**C1**) Microglial and macrophagic proliferation in cortex and white matter (detail in **C2**). Few scattered T lymphocytes are seen in the leptomeninges (**D**).

SARS-CoV-2 detection in the brain and lung tissues

In order to investigate SARS-CoV-2 infection in the nervous system, tissue samples of the brain and brainstem were processed for immunostaining against SARS-CoV-2 spike protein (SP). Lung was also analyzed as a positive control sample. As expected, SP was present in groups of nearby cells in the lung (**Fig 3 B,b**). Among brain and brainstem areas, we observed staining for SP in the ChP localized along epithelium, mainly in the apical cytoplasm (**Fig 3 D,d and Supp Fig 3**). Considering that ChP extends within each ventricle in the brain, not surprisingly we detected SP positive cells, to a lesser extent, in the ependyma of the lateral ventricle (**Supp Fig 3B and 3b**). We also observed scarce cells positive for SP in the cortex (**Fig 3 F,f**).

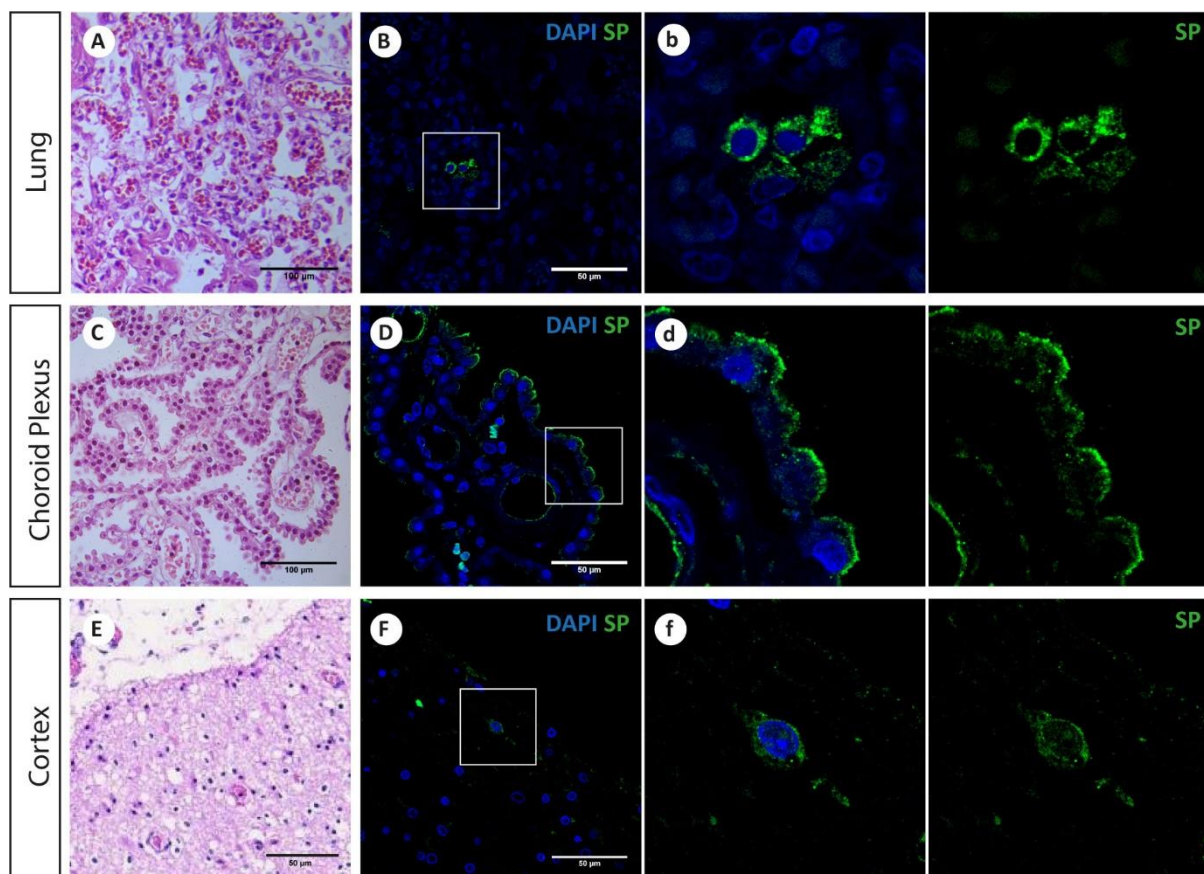


Figure 3: Light and immunofluorescence staining photomicrographs for spike protein (SP) in the brain (cerebral cortex and choroid plexus) and lung. (A) Lung tissue with marked pneumonitis. **(B, b)** SARS-CoV-2 infected cells in the lung detected by SP. **(C)** Choroid plexus of the cerebral lateral ventricle. Note vascularized and ramified papillary structures covered with a simple cuboidal epithelium. **(D, d)** SARS-CoV-2 infected cells in the choroid plexus detected by SP. **(E)** Cerebral cortex with marked edema. **(F, f)** SARS-CoV-2 infected cells detected in the cortex by SP. (A, C, E - H&E).

Discussion

We reported the histopathological *post-mortem* findings of a 1-year and 2-months-old infant that died of COVID-19. We observed a severe pneumonitis and a massive cerebral hypotrophy and edema caused by hypoxic encephalopathy (a co-morbidity that might have contributed to the bad outcome of COVID-19), secondary to the prolonged respiratory disease and the episodes of seizures. We also demonstrated that SARS-CoV-2 substantially infected the choroid plexus but very mildly the cortex.

The cause of death was a severe pneumonitis with diffuse bronchiolar and alveolar damage, together with massive pancreatic ischemic necrosis secondary to a large vessel thrombosis, both reported in patients infected with the SARS-CoV-2 (8,9). Besides the thrombosis found in the pancreas, the infant presented multiple thrombotic events in several organs. *Post-mortem* studies have shown the presence of thrombosis and microangiopathy in the small vessels of major organs, including the lungs (8,10). Liver steatosis could be associated with the anti-convulsive drugs taken by this child.

Another hallmark of severe COVID-19 is the overproduction of proinflammatory cytokines which leads to systemic inflammation (11) and contributes to thrombus formation (12,13). We observed leukocytes infiltration, hyaline membranes and plugs of plasma proteins and cellular debris in the lung parenchyma but lymphoid depletion was also detected in lymphoid tissues, as previously reported (8).

The damage of the central nervous system (CNS) reported here could be related to hypoxia, secondary to both the prolonged pneumonitis and the intermittent episodes of seizures. The differential diagnosis with Alpers-Huttenlocher syndrome (which has features of anoxic encephalopathy and liver steatosis), cannot be ruled out (14). Together with severe nerve loss, the reactive gliosis observed is expected in both encephalopathies, particularly in the cortex, as well as the macrophagic activity. However, an excessive microgliosis and white matter gliosis was unexpected and could be related to SARS-CoV-2 infection in the CNS. In fact, it has been reported increased plasma levels of GFAP and neurofilament light chain protein in COVID-19 severe patients, which might explain the outcomes of CNS injury related to SARS-CoV-2 infection (15) and the neurological signs and symptoms. Systemic lymphoid depletion, as mentioned above, could also explain the fact that leptomeningitis in this case (described for the first time in children in association with the SARS-CoV-2 infection) coursed with very mild lymphocytic infiltration.

Despite the suggested neurological infection, the route of SARS-CoV-2 entry into the CNS is still under debate. Recently, it was demonstrated infection by SARS-CoV-2 associated with local ischemic infarcts in the adult human brain (16). SARS-CoV-2 uses the angiotensin-converting enzyme 2 (ACE2) as the main entry in the host cells. ACE2 is mainly expressed in the heart, kidney, small intestine, testis, placenta, eye and vessels. The brain presents negligible amounts of ACE2 protein, except for the choroid plexus, which exhibits high expression of ACE2 (17,18). Indeed, we found considerable immunostaining for SP in choroid plexus epithelium and, to a lesser extent, in ependymal cells, but it was scarce in other brain areas, such as the cortex, probably due to a very mild infection.

Choroid plexus has a single epithelial layer attached by tight junctions that participates in the blood-CSF barrier (19–21). A study evidenced SARS-CoV-2 particles in endothelial cells, as well as inflammation (22). Given the essential role of endothelium in vascular permeability homeostasis, endothelium dysfunction caused by SARS-CoV-2 infection may contribute to the thrombo-inflammatory process resulting in vasculopathy (23). Thus, infection of the choroid plexus could enable SARS-CoV-2 to invade CNS and disrupt the CSF barrier.

Our findings are in accordance with previous works *in vitro* showing choroid plexus infection by SARS-CoV-2 in brain organoids (24,25). The authors demonstrated that SARS-CoV-2 has minimal tropism for neurons and glial cells but promotes the brain-CSF barrier breakdown (24). Likely, the deleterious findings in the *post-mortem* brain tissues was due to the previous encephalopathy added to the entry of immune cells and cytokines through the disrupted blood-CSF barrier. Supporting this concept, SARS-CoV-2 RNA was found in the cerebrospinal fluid of one patient with COVID-19 encephalitis (4).

Here we reported several multisystemic histopathological alterations caused by SARS-CoV-2 in an infant. Severe SARS-CoV-2 cases in children are rare but concerning because they may result in death or sequelae in many cases. The differences of SARS-CoV-2 behavior between children and adults are not clear, but they seem to share hallmarks, including inflammation, thrombosis, and secondary tissue hypoxia. Indeed, our histopathological findings showed all these aspects in addition to meningitis. We also showed that SARS-CoV-2 substantially infects the choroid plexus *in vivo*. Although SARS-CoV-2 does not diffuse effectively within the CNS it might profoundly damage it, since the excessive microgliosis observed in this case was unexpected in anoxic encephalopathy. This report elucidates many aspects of SARS-CoV-2 infection *in vivo* contributing to the search for clinical and pharmacological strategies against COVID-19.

Acknowledgements

We thank Leticia Souza for technical support in confocal images acquisition; Diego Santos and Heliomar Pereira Marcos for immunohistochemical staining technique. Financial support (not specifically for COVID-19 studies) was provided by the Foundation for Research Support in the State of Rio de Janeiro (FAPERJ); the National Council of Scientific and Technological Development (CNPq) and Coordination for the Improvement of Higher Education Personnel (CAPES), in addition to intramural grants from D'Or Institute for Research and Education.

Competing interests

The authors declare no competing interests.

References

1. Worldometer. Coronavirus Cases [Internet]. 2020. Available from: worldometers.info/coronavirus
2. Mao L, Wang M, Chen S, He Q, Chang J. Neurological Manifestations of Hospitalized Patients with COVID-19 in Wuhan , China : a retrospective case series study. 2020;
3. Montalvan V, Lee J, Bueso T, Toledo J De, Rivas K. Neurological manifestation of Covid-19 and other coronavirus infections: A systematic review. *Clin Neurol Neurosurg.* 2020;194(January):105921.
4. Moriguchi T, Harii N, Goto J, Harada D, Sugawara H. A first case of meningitis/encephalitis associated with SARS-Coronavirus-2. *Int J Infect Dis.* 2020;94(January):55–8.
5. Xu J, Zhong S, Liu J, Li L, Li Y, Wu X, et al. Detection of Severe Acute Respiratory Syndrome Coronavirus in the Brain : Potential Role of the Chemokine Mig in Pathogenesis. *Clin Infect Dis.* 2005;41:1089–96.
6. Solomon IH, Normandin E, Bhattacharyya S, Mukerji SS, Keller K, Ali AS, et al. Neuropathological Features of Covid-19. *N Engl J Med.* 2020;1–4.
7. Pires ARC, Andreiuolo F da M, Souza SR De. TMA for all : a new method for the construction of tissue microarrays without recipient paraffin block using custom-built needles. *Diagn Pathol.* 2006;5:1–5.
8. Hanley B, Naresh KN, Roufousse C, Nicholson AG, Weir J, Cooke GS, et al. Histopathological findings and viral tropism in UK patients with severe fatal COVID-19 : a post-mortem study. *The Lancet Microbe* [Internet]. 2020;5247(20). Available from: [http://dx.doi.org/10.1016/S2666-5247\(20\)30115-4](http://dx.doi.org/10.1016/S2666-5247(20)30115-4)

9. Duarte-Neto AN, Monteiro RA de A, Silva LFF da, Malheiros DMAC, Oliveira EP de, Filho JT, et al. Pulmonary and systemic involvement of COVID-19 assessed by ultrasound-guided minimally invasive autopsy. *Histopathology*. 2020;(May 22):0–2.
10. Carsana L, Sonzogni A, Nasr A, Rossi RS, Pellegrinelli A, Zerbi P, et al. Pulmonary post-mortem findings in a series of COVID-19 cases from northern Italy: a two-centre descriptive study. 2020;(January).
11. Pedersen SF, Ho Y-C. SARS-Cov-2: a storm is raging. *J Clin Invest*. 2020;2202–3.
12. Tufan A, Guler AA, Matucci-Cerinic M. COVID-19 , immune system response , hyperinflammation and repurposing antirheumatic drugs. *Turkish J Med Sci*. 2020;50(March):620–32.
13. Lazzaroni MG, Piantoni S, Masneri S, Garrafa E, Martini G, Tincani A. Coagulation dysfunction in Covid-19: The interplay between inflammation, viral infection and the coagulation system. *Blood Rev [Internet]*. 2020;100745. Available from: <https://doi.org/10.1016/j.blre.2020.100745>
14. Simonati A, Filosto M, Savio C, Tomelleri G, Tonin P, Dalla B, et al. Features of cell death in brain and liver , the target tissues of progressive neuronal degeneration of childhood with liver disease (Alpers-Huttenlocher disease). 2003;57–65.
15. Kanberg N, Ashton NiJ, Andersson L-M, Yilmaz A, Lindh M, Nilsson S, et al. Neurochemical evidence of astrocytic and neuronal injury commonly found in COVID-19. *Neurology*. 2020;(Jun 26):0–17.
16. Song E, Zhang C, Israelow B, Lu-Culligan A, Prado AV, Skriabine S, et al. Neuroinvasion of SARS-CoV-2 in human and mouse brain. *bioRxiv [Internet]*. 2020; Available from: <https://doi.org/10.1101/2020.06.25.169946> .
17. Hikmet F, Méar L, Edvinsson Å, Micke P, Uhlén M, Lindskog C. The protein expression profile of ACE 2 in human tissues. *Mol Syst Biol*. 2020;(16):1–16.
18. Chen R, Wang K, Yu J, Chen Z, Wen C, Xu Z. The spatial and cell-type distribution of SARS-CoV-2 receptor ACE2 in human and mouse brain. *bioRxiv [Internet]*. 2020; Available from: <https://doi.org/10.1101/2020.04.07.030650>
19. Lun MP, Monuki ES, Lehtinen MK. Development and functions of the choroid plexus – cerebrospinal fluid system. *Nat Publ Gr [Internet]*. 2015;(July):1–13. Available from: <http://dx.doi.org/10.1038/nrn3921>
20. Milton Brightman. The Intracerebral Movement of Proteins Injected into Blood and Cerebrospinal Fluid of Mice. *Prog Brain Res*. 1957;36–7.
21. Hilhorat TH, Davis DA LBJ. Two morphologically distinct bloodbrain barriers preventing entry of cytochrome c into cerebrospinal fluid. *Science (80-)*. 1973;(80):76–8.
22. Varga Z, Flammer AJ, Steiger P, Haberecker M, Andermatt R, Zinkernagel AS, et al. Correspondence Endothelial cell infection and endotheliitis in. *Lancet*. 2019;395(May):1417–8.

23. Mcgonagle D, Donnell JSO, Sharif K, Emery P, Bridgewood C. Viewpoint Immune mechanisms of pulmonary intravascular coagulopathy in COVID-19 pneumonia. *Lancet Rheumatol* [Internet]. 2020;2019(20):1–9. Available from: [http://dx.doi.org/10.1016/S2665-9913\(20\)30121-1](http://dx.doi.org/10.1016/S2665-9913(20)30121-1)
24. Pellegrini L, Albecka A, Mallery DL, Kellner MJ, Paul D, Carter AP, et al. SARS-Cov-2 infects brain choroid plexus and disrupts the blood-CSF-barrier. *bioRxiv*. 2020;1–14.
25. Jacob F, Pather SR, Huang W, Zheng S, Wong H, Zhou H. Human Pluripotent Stem Cell-Derived Neural Cells and Brain Organoids Reveal. *bioRxiv*. 2020;1–52.